Journal of Molecular Spectroscopy xxx (2017) xxx–xxx

Contents lists available at ScienceDirect

Journal of Molecular Spectroscopy

journal homepage: www.elsevier.com/locate/jms

The equilibrium structure of hydrogen peroxide

Joshua H. Baraban [a,*], P. Bryan Changala [b], John F. Stanton [c]

[a] Department of Chemistry, Ben-Gurion University of the Negev, Beer-Sheva 84105, Israel
[b] JILA, National Institute of Standards and Technology and Department of Physics, University of Colorado, Boulder, CO 80309, USA
[c] Quantum Theory Project, Depts. of Chemistry and Physics, University of Florida, Gainesville, FL 32611, USA

ARTICLE INFO

Article history:
Received 12 July 2017
In revised form 27 September 2017
Accepted 28 September 2017
Available online xxxx

ABSTRACT

The equilibrium structure of hydrogen peroxide is completely determined for the first time. Recent isotopically substituted data is combined with the results of rovibrational variational calculations to yield a complete semi-experimental structure, which is in excellent agreement with high level *ab initio* calculated structures. In addition to numerically exact variational calculations, we also investigate the accuracy of approximate rovibrational predictions based on second order vibrational Møller-Plesset perturbation theory with curvilinear coordinates.

1. Introduction

Large amplitude motion is a commonly occurring but still under appreciated molecular behavior. A well-known example is the torsional tunneling found in the ground state of hydrogen peroxide [1]; despite extensive work on this fundamental reactive molecule, its equilibrium structure has never been determined precisely. One might have guessed that early attempts to derive the structural parameters of H_2O_2 from rotational spectroscopy were chiefly hampered by insufficient data (four independent coordinates but only three rotational constants [2–8]), but in fact the main difficulty was the very large difference between r_0 and r_e for this decidedly floppy molecule. Significant progress was made on this problem by Koput [9,10] but, without additional isotopic data, a complete structure could not be obtained. Sufficient information [11–15] now allows a complete semi-experimental equilibrium structure [16] to be determined.

The semi-experimental structure requires theoretical input from rovibrational calculations, for which we turn to numerically exact variational methods. These results also serve as a useful reference for assessing the performance of approximate rovibrational methods, in particular curvilinear coordinate vibrational second order Møller-Plesset perturbation theory (VMP2) [17–19] and a recently developed extension for $J > 0$ rovibrational calculations [20]. The use of a curvilinear coordinate description makes this method applicable to molecules exhibiting large amplitude nuclear motion. Hydrogen peroxide, as the simplest torsionally isomerizing system, is therefore a particularly relevant benchmark.

2. Methods

Semi-experimental equilibrium rotational constants (B_e^{se}) were calculated by subtracting *ab initio* rotation-vibration parameters ($B_e - B_0$, frequently approximated in perturbation-theory-based methods as $-\frac{1}{2}\sum_i \alpha_i^B$) from the experimentally observed rotational constant values [11–15]. These rovibrational zero-point motion corrections were obtained with several treatments of the nuclear motion (second order vibrational perturbation theory (VPT2) [21], second-order vibrational Møller-Plesset theory (VMP2) [20], and variational) on potential energy surfaces (PES) using various levels of electronic structure theory [22,23]. Variational calculations on the "V+C+R+H" PES of Ref. [23] achieved the best agreement with the experimentally measured rovibrational levels, and so rotation-vibration parameters using this surface were employed for the structure fit. Electronic contributions to the rotational constants were also computed [24,25] at frozen core CCSD(T)/aug-cc-pVTZ.

In addition to the PES, the VMP2 calculations require two major inputs: the internal vibrational coordinate system and the choice of molecule body-fixed frame embedding. For the former, we employed a curvilinear reaction path coordinate system, which is necessary to properly treat a large amplitude motion, multi-well system within the framework of VMP2. Multiple frame embeddings were used, including a standard Eckart frame tied to the planar *trans* transition state geometry and a moving Eckart frame tied to the instantaneous principal axis system along the torsional isomerization coordinate. We also investigated the effects of including the rotational degrees of freedom in the self-consistent field (SCF) portion of the calculation, making it an explicitly *ro*vibrational SCF. We will refer to the perturbation theory results associ-

* Corresponding author.
E-mail address: jbaraban@bgu.ac.il (J.H. Baraban).

https://doi.org/10.1016/j.jms.2017.09.014
0022-2852/

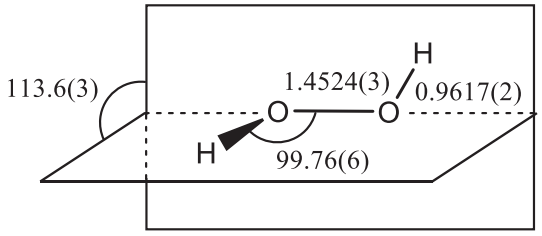

Fig. 1. The molecular r_e^{se} structure of H_2O_2. Bond lengths in Å, angles in degrees.

Table 1
H_2O_2 geometries. Bond lengths in Å, angles in degrees. The experimental structure is a semi-experimental equilibrium structure, r_e^{se}, obtained by correcting experimental rotational constants for zero-point rotation-vibration effects calculated *ab initio*.

Parameter	Calc.[a]	r_e^{se}	Ref. [10]	Ref. [23]	r_0
r_{OH}	0.9623	0.9617(2)	0.965(5)	0.9628	0.9675(9)
r_{OO}	1.4515	1.4524(3)	1.452(5)	1.4509	1.461(1)
∠OOH	100.07	99.76(6)	100(1)	100.09	100.07(25)
∠HOOH	113.17	113.6(3)	112(1)	112.81	119(1)

[a] Extrapolation of optimized all electron CCSD(T)/cc-pCVTZ–5Z geometries, supplemented by a higher order perturbative quadruples correction calculated with the pCVTZ basis set and the frozen core approximation.

ated with this approach as "RVMP2". Further details of the VMP2/RVMP2 calculations are discussed in Appendix A.

All calculations were performed with the CFOUR [26] and NITROGEN [27] program systems, using atomic masses.

3. Results and discussion

3.1. Equilibrium structure

Fig. 1 shows the semi-experimental equilibrium molecular structure, which is compared with an extrapolated *ab initio* structure [28,29] in Table 1. We wish to emphasize the large differences between the r_e and r_0 structures reported in Table 1; as noted by Koput [10], it is critical to account for the effects of the large amplitude torsional motion. In general, the effects of zero point motion on the spectroscopic determination of molecular structures are under-appreciated, and in this particular case the vibration-rotation corrections amount to a few percent of the rotational constants. Perturbative quadruples have a surprisingly large effect on the torsional angle (nearly 0.3°) and the valence bond angle (almost 0.15°), presumably due to the interaction of the adjacent lone pairs.

Much of the debate in the literature over the structure of H_2O_2 has revolved around the choice of a reasonable value for r_{OH}, so that the remaining parameters could be determined by the existing rotational constant data. Two predictions validated by the current work are a) that this (r_e) bond length is more similar to that in water [30] (0.95781(03) Å, [31,32]), than to that of the hydroxyl radical (0.96966 Å, [33]), and b) that the r_0 value is approximately 0.967 Å. [5,34] We rationalize this by noting that the hybridization in H_2O_2 is clearly more similar to H_2O than to OH.

3.2. Comparing variational and VMP2 predictions

The predicted energies for the small amplitude fundamental levels and torsional overtones are summarized in Tables 2 and 3, respectively. The root-mean-square difference between the perturbative VMP2 and reference variational energies is 0.32 cm^{-1} for the small amplitude fundamentals and < 0.01 cm^{-1} for the lowest 5 torsionally excited states. These errors are comparable to or smaller than the corresponding differences between the variational predictions and the observed values. In other words, the errors introduced by the VMP2 approximations are less important than errors in the Born-Oppenheimer potential energy surface. The small VMP2 errors, especially in the torsion overtone series, further indicate that the zeroth order picture of separable vibrations captures accurately all the important features of the vibrational dynamics. This success is entirely dependent on the use of the reaction path coordinate system. Other choices of coordinates would fare worse with this mean-field-based approach [19].

Table 2
Predicted fundamental frequencies of the five small amplitude vibrations of H_2O_2. All values are in cm^{-1}.

Mode	Description	VMP2	Var.	Obs.[a]
ν_3	OO stretch	865.77	865.65	865.94
ν_6	asym. bend	1264.77	1264.78	1264.58
ν_2	sym. bend	1394.43	1394.36	1395.88
ν_1	sym. OH stretch	3609.73	3609.20	3609.8
ν_5	asym. OH stretch	3611.05	3610.49	3610.66

[a] Refs. [35–38].

Table 3
Predicted energies of the pure torsional levels, using the (n, τ) labeling convention. All values are in cm^{-1}.

(n, τ)	VMP2	Var.	Obs.[a]
(0,1)	0	0	0
(0,4)	11.01	11.01	11.44
(1,1)	256.41	256.40	254.55
(1,4)	371.26	371.24	370.89
(2,1)	570.32	570.32	569.74
(2,4)	776.43	776.41	776.12

[a] Ref. [8].

Turning to rovibrational aspects, Table 4 compares the calculated zero-point vibrational corrections to rotational constants for a variety of methods against our variational benchmark. We focus on the predicted zero-point corrections, rather than the absolute ground state values, because it is the corrections that are needed to determine a semi-experimental equilibrium structure. Taking all three rotational constants into account, the most accurate approximate method is the RVMP2 approach using the Eckart-LAM embedding. The significant difference between this and the standard VMP2 predictions with the same Eckart-LAM embedding is in the *A* constant shift. This implicates torsion-rotation interactions about the *a* axis as the primary difficulty, as expected. The improved accuracy of the RVMP2 vs. VMP2 predictions is a consequence of the fact that the torsional factor of the zeroth order RVMP2 wavefunction can adapt to angular momentum about the *a*-axis in the rotational wavefunction.

We also note that the VMP2 and RVMP2 calculations are uniformly more accurate than VPT2 predictions. The multi-well nature of the H_2O_2 PES and the resulting anharmonicity of the torsional degree of freedom are treated less than optimally by

Table 4
Comparison of calculated zero-point vibrational shifts to rotational constants. All values are in MHz. The ground state rotational constants for variational, VMP2, and RVMP2 predictions were determined solely from $J = 1$ energies, ignoring centrifugal distortion effects. "Eckart" refers to single-reference Eckart embedding using the *trans* transition state, and "Eckart-LAM" refers to the moving Eckart frame along the isomerization path. (See Appendix A for details.)

Parameter	Var.	VMP2 (Eckart)	VMP2 (Eckart-LAM)	RVMP2 (Eckart-LAM)	VPT2
$A_e - A_0$	2346	2265	2419	2342	2731
$B_e - B_0$	281	290	260	260	320
$C_e - C_0$	507	520	530	529	445